BJET
(Bayero Journal of Engineering and Technology)
https://bjet.ng/index.php/jet
Research Article
2026, Vol. 21 (2), 1-6

Monopole Antenna with Ultra-Wideband Characteristics for Broadband Communication Systems

Babale S. A.[1], Lawan S. H.[2*], Lawal M. B.[2], Auwalu A. A[2], Babani S.[2] and Falalu I. S.[3]

[1]Department of Electronics and Telecommunications Engineering, Ahmadu Bello University, Zaria – Nigeria.

[2]Department of Telecommunication Engineering, Bayero University, Kano – Nigeria

[3]Department of Physical Planning, Nigerian Collage of Aviation Technology, Zaria.

[*]Corresponding author email: shlawan.ele@buk.edu.ng

Received: 31-12-2025
Revised: 08-01-2026
Accepted: 20-04-2026
Published: 21-04-2026

Abstract: *This study presents the design, simulation and performance evaluation of a transparent Ultra-wideband (UWB) monopole antenna employing a shrinked-trapezoidal defected ground structure (DGS) fabricated on a quartz substrate. The antenna was modeled and optimized using CST Studio Suite. A transparent quartz glass substrate was selected due to its low loss tangent and optical clarity, while a silver mesh was used as the conductive layer to preserve transparency and enhance conductivity. The design supports deployment on see-through surfaces such as glass panels, windshields, and display screens. Simulation results show an impedance bandwidth of 157%, spanning 1.52–12.58 GHz, which meets UWB specifications and enables applications in high-data-rate wireless communication, radar sensing, and Internet of Things (IoT) systems. Radiation characteristics including gain, efficiency, and polarization were analyzed, confirming stable omnidirectional patterns*

Key words: Monopole antenna, quartz substrate, UWB antenna, and defected ground

1 Introduction

Due to its capacity for high data transmission rate, minimal power consumption, and resilience in multipath circumstances, Ultra-wideband (UWB) technology has grown significant attention. UWB antennas are vital for supporting modern wireless applications including radar, medical imaging, and indoor locations. This is due to the wide impedance bandwidths possess, they also have a consistent radiation pattern, and compact geometries (Kalteh et al., 2012; Ishfaq et al., 2021; Toktas and Turkmen, 2023; Luo et al., 2022).

Different type of antenna shapes, including planar monopoles, dipoles, slots, and patch-based topologies have been examined recently in UWB research. Each of these configurations is optimal for distinct design goals, such as bandwidth increase, miniaturization, or polarization control (Zhu et al., 2023; Babale et al., 2022; Yen et al., 2023; Dwivedi et al., 2023).

Having a wide impedance bandwidth while at the same time keeping compactness and radiation efficiency is still a difficulty, though. The opaque metallic substrates of many typical UWB antennas sometimes hinder their integration into visually pleasant or transparent surfaces like windows or car windshields (Paracha et al., 2019). By designing a transparent UWB monopole antenna based on a Quartz substrate incorporated with a trapezoidal Defective Ground Structure (DGS), this paper solves this constraint.

Many works related to bandwidth improvement in UWB antenna systems have been the focus of some Researchers. A planar UWB antennas with defected ground structures that obtained bandwidths over 10 GHz were demonstrated by Hosseini et al. (2008). A CPW-fed slot antenna with dual circular polarization and a 153% impedance bandwidth was also demonstrated by Li et al. (2019). Ramya and Rani (2022) proposed a CPW-fed dodecagon monopole with a fractional bandwidth of 135.96%, whereas Adamu et al. (2018) recommended a high-gain, modified antipodal Vivaldi antenna that could operate from 2.15 to 11 GHz. Furthermore, printed metasurface-based antennas (Khadar et al., 2021) and

circular-shaped monopole antennas (Singhal and Singh, 2016) have been proposed to boost radiation stability and the antenna bandwidth.

From the same study, the gain and efficiency have also been improved by the use of metamaterial integration. A stacked patch antenna proposed by Shakib et al. (2010) obtained a gain of 7.1 dBi, and a bandwidth of 63.2%. However, standard opaque boards were employed in the majority of these designs. In contrast, a transparent quartz-based structure suited for both electromagnetic and optical performance is proposed in this current study. Also, the defected ground structure (DGS) as one of the famous techniques in antenna bandwidth improvement is introduced on a quartz substrate of this work, to improve the limited bandwidth shortcomings.

2 Antenna Design and Structure

2.1 The Conventional Microstrip Patch Antenna Model

The initial microstrip patch antenna model was adopted from (Bala et al., 2021), and it was designed to have a rectangular form on a Quartz substrate with an operational frequency band of 5.82 GHz to 6.03 GHz, a dielectric constant of 4.4, a loss tangent of D = 0.02, and a substrate thickness of 1.6 mm. Because of its low loss and accessibility on the market, the substrate was selected for this antenna design. At high frequencies, the relative permittivity of Quartz substrate is predicted to be frequency-dependent, decreasing as frequency increases. The dielectric constant's frequency behavior in the Quartz substrate case is dependent on the materials used to make it, such as glass and epoxy resin (Babale et al; 2022).
As seen in Fig. 1(a), the initial antenna patch size 38.5 x 41.2 mm. The ground plane and radiating patch, which are the two conducting components of this antenna that were etched at the top of the board, are composed of silver mesh conductor. Fig. 1(b) shows the back view of the MPA and Fig. 1(c) illustrates the simulated S11 plot of the antenna reflection coefficient as a function of frequency. With a bandwidth of 200MHz and a frequency range of 5.82GHz to 6.03GHz, this primary antenna design operates below the -10 dB limit with return loss value of -27.5 dB, at 6.0 GHz resonance frequency.

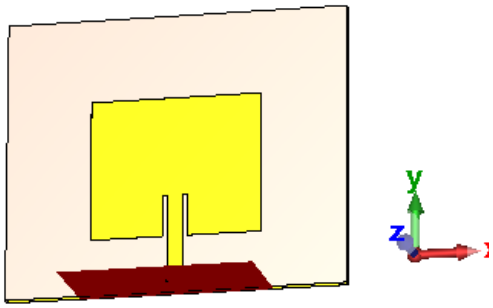

(a) Front view of the MPA

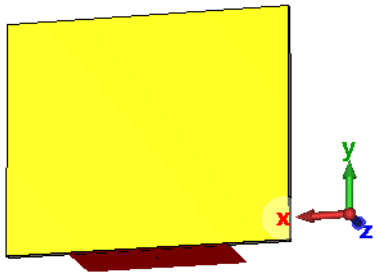

(b) Back view of the MPA

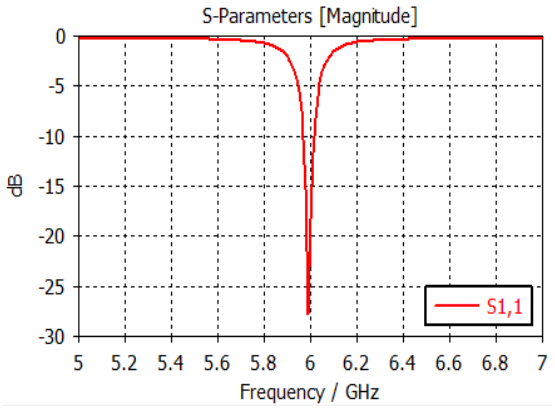

(b) S11 Simulated of the MPA

Figure 1: Geometry of the Conventional MPA; (a) the front view of the MPA antenna, (b) the Back view of the MPA antenna and (c) the S11 of the MPA antenna

2.2 The Ultrawideband Antenna

A conventional MPA antenna was used as the initial point for the design of the rectangular monopole radiator. It was initially chamfered at the top corner of both ends which helped to reduce the size without reducing antenna performance. A shrinked-trapezoidal defected structure is created on the ground plane in order to increase impedance bandwidth, which enhance capacitive coupling between the

ground and radiator, thereby modifying the current distribution. which was the key that makes up the proposed wideband antenna architecture. Similar to the MPA design, the wideband antenna was designed on a Quartz substrate that has a loss tangent of 0.004, thickness of 0.7 mm, and a relative permittivity (ε_r) of 3.75. A 50-ohm microstrip line was used as feeding line in order to obtain an exceptional impedance matching. A Computer Simulation Technology (CST) Microwave Studio 2023 was used for all the simulations, and parametric optimizations were applied to the upper ground edge (L3) and the ground defect length (L2) to achieve maximum bandwidth. The substrate dimension used is 39.64mm x 37.46mm. Other patch dimensions of the UWB MPA are listed in table 1.0.

Table 1.0: Optimized Antenna Parameter

Parameter	Values
WP	28.28
LP	23.1
WF	4.61
LF	16.56
WG	0.018
LG	4.55
K	8.4
L2	13.44
BR	12.12

Where W_P, W_F and W_G are the widths of the patch, feed and the ground respectively. So also, L_P, L_F and L_G are the respective lengths of the lengths of the patch, feed and the ground. K and BR are the port extension coefficient and the blend radius respectively.

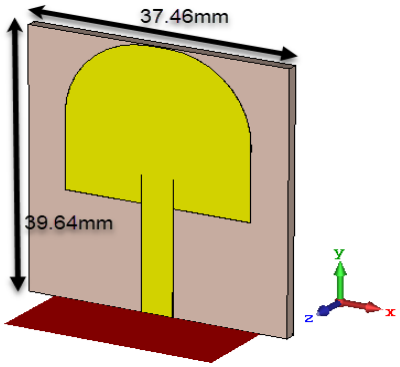

(c) the front view of the UWB antenna

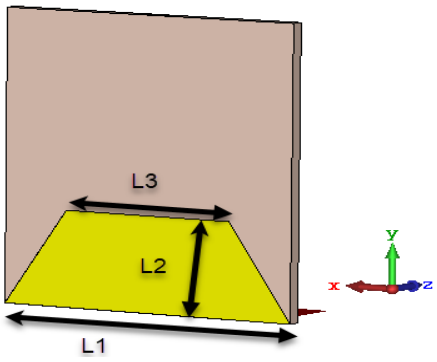

(b) the back view of the UWB antenna

Figure 2: Geometry of the proposed UWB antenna.

3 Simulation Setup

A transient solver embedded in the CST was used for simulation. An open boundary conditions were utilized in CST Studio Suite, to run the simulation of the antenna. For the excitation, a single 50 Ω connection was employed. Important antenna metrices like the gain, radiation efficiency, impedance bandwidth, and the reflection coefficient (S11). Were targeted for the optimization. To cover the full UWB band, frequency sweeps were carried out between a frequency of 1 to 13 GHz.

4 Results and Discussion

4.1 Coefficient of Reflection (S11)

The optimized S11 plot shown in Fig. 3 indicates three major resonances at 3.2 GHz, 5.8 GHz, and 10 GHz. The simulated -10 dB bandwidth extends from 1.52 GHz to 12.58 GHz, corresponding to a fractional bandwidth of 157%. This result outperforms many previously reported UWB monopole antennas, demonstrating the effectiveness of the DGS in widening bandwidth.

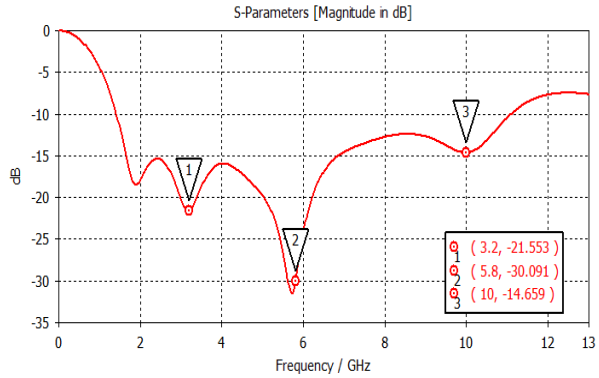

(a)

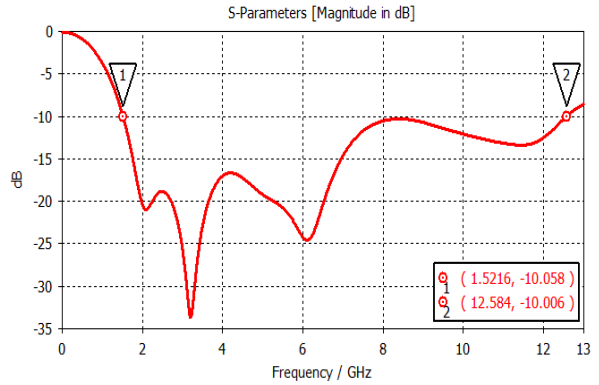

(b)

Figure 3: Simulated reflection coefficient S11 in dB vs the frequency in GHz. Plot (a) Initial design and (b) Optimized design.

4.2 Patch Size Variation

A parametric study revealed that variations in antenna length (26–30.16 mm) had minimal impact on the depth of the S11, while the variations in the width of the antenna from 30.79 to 39.16 mm influences the high-frequency bandwidth expansion. From the results presented in Fig. 4, it can be observed that increasing the patch width improves the impedance matching and the overall bandwidth of the UWB antenna.

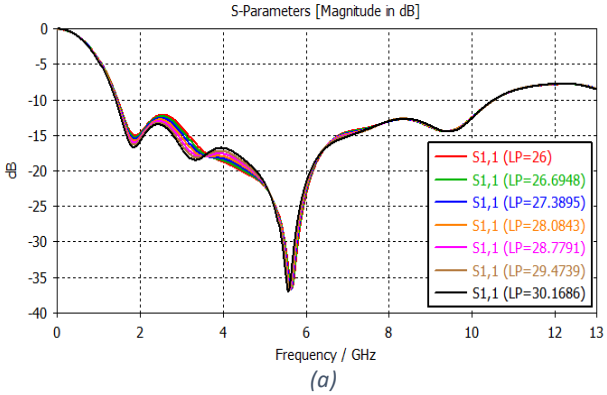

(a)

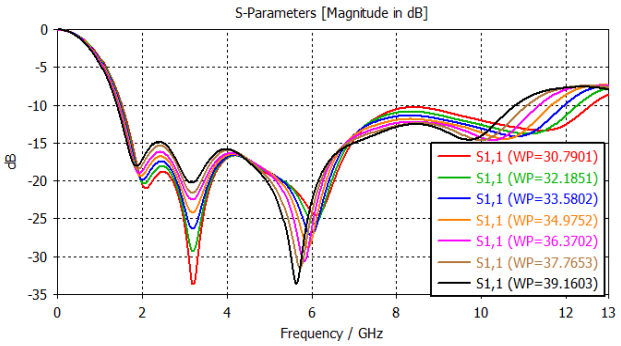

(b)

Figure 4: Effect of variation of the UWB antenna parameters on the S11. Plot (a) Variation in length (b) variation in width

4.3 Radiation Pattern and Gain

Fig. 5 shows the simulated 1-D far-field radiation patterns of the proposed antenna in the elevation plane, at 3.2 GHz, 5.8 GHz, and 10 GHz. It shows both the co-polarized and the cross-polarized patterns.

At a frequency of 3.2 GHz, the antenna shows a clear radiation pattern with a strong co-polarized field and a cross-polarized component that is significantly weaker. The major lobe points around 180°, which suggests that the broadside radiation is stable and the polarization purity is good at the lower operating frequency. The low cross-polarization level indicates little undesirable field components, which is beneficial for efficient radiation and minimal interference.

The radiation properties at 5.8 GHz are similar as the one presented at 3.2 GHz. The co-polarized part is still the strongest at all elevation angles, whereas the cross-polarized part is still quite weak. But there is a little shift in the form of the beam and the formation of small sidelobes, which can be explained by the fact that the antenna is electrically larger at this frequency. Nonetheless, the antenna offers very good directivity and polarization discrimination.

At the 10 GHz frequency, the radiation pattern gets wider and more uniformly spread out. The antenna still functions effectively, but the spacing between the co-polarized and cross-polarized sections is smaller than it is at lower frequencies. This data demonstrates greater cross-polarization and pattern distortion at elevated frequencies, probably arising from higher-order mode excitation and enhanced surface current fluctuations. Even yet, the antenna still functions well in terms of radiation across the complete operating band.

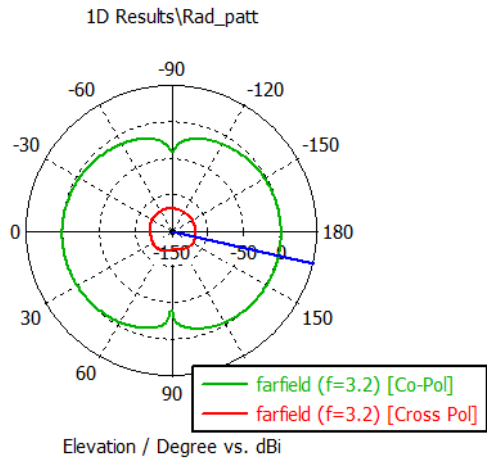

(a)

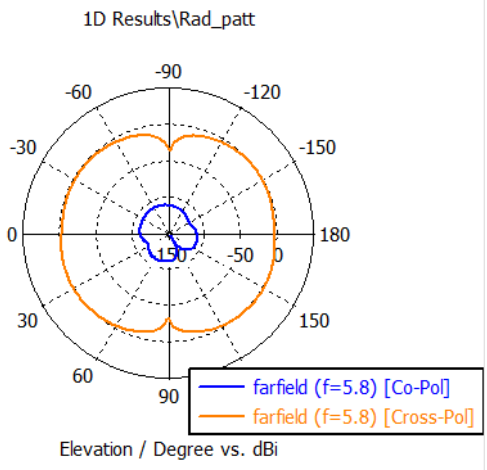

(b)

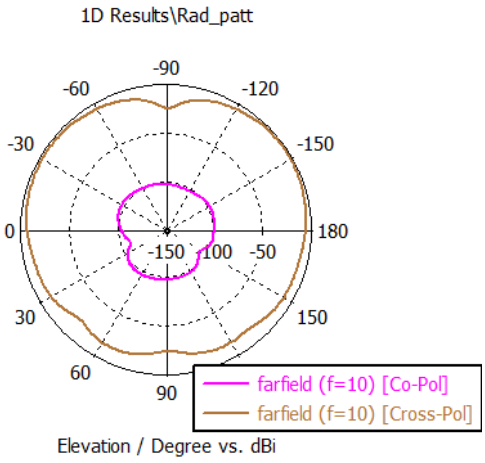

(c)

Figure 5: Radiation pattern of the proposed UWB antenna at (a) 3.2 GHz (b) 5.8 GHz (c) 10 GHz

The overall simulated results obtained in this work reveal that, the antenna studied has a good directional radiation and significant co-polarization dominance at lower and mid-band frequencies. However, at higher frequencies, the polarization purity slowly grows worse. These qualities as an indication that the antenna is appropriate for wideband operation, especially in a situation where stable radiation patterns and low cross-polarization are needed over a large range of frequencies.

5 Conclusion

A transparent UWB monopole antenna based on a Quartz substrate with a trapezoidal defected ground structure have been presented. The proposed design achieved a 157% impedance bandwidth from 1.52–12.58 GHz, stable omnidirectional radiation, and strong polarization characteristics. The use of quartz substrate and silver mesh conductor makes the antenna suitable for transparent installations such as windows and vehicular windshields. The design demonstrates significant potential for integration in smart infrastructure, vehicular communication, and IoT applications, representing a step forward in the development of transparent wireless communication technologies. While this research has successfully demonstrated the design and performance of a monopole antenna with ultra-wideband characteristics for broadband communication systems, several avenues remain open for further investigation. Future studies could focus on the fabrication of the Antenna and compare its measured results and the simulated ones.

References

Adamu, S.A., Masri, T., Abidin, W.A.W.Z., Ping, K.H. and Babale, S.A. (2018) 'High-gain modified antipodal Vivaldi antenna for ultra-wideband applications', Journal of Telecommunication, Electronic and Computer Engineering, 10(1–12), pp. 55–59.

Babale, S.A., Paracha, K.N., Ahmad, S., Abdul Rahim, S.K., Yunusa, Z., Nasir, M., Ghaffar, A. and Lamkaddem, A., 2022. A recent approach towards fluidic microstrip devices and gas sensors: a review. Electronics, 11(2), p.229.

Bala, S., Yunusa, Z. and Babale, S.A., 2021. Design and analysis of a rectangular microstrip patch antenna using different dielectric materials for sub-6GHz 5G applications. Nigerian Journal of Engineering, 28(2), pp.48-57.

Dwivedi, R.P., Kommuri, U.K., Das, S., Lakrit, S. and Goyal, V. (2023) 'Design of low profile high gain antenna using loop-based wideband artificial magnetic conductor for UWB applications', International Journal of Microwave and Wireless Technologies, 15(3), pp. 502–512.

Hosseini, S.A., Atlasbaf, Z. and Forooraghi, K. (2008) 'Two new loaded compact planar ultra-wideband antennas using defected ground structures', Progress in Electromagnetics Research B, 2, pp. 165–176.

Ishfaq, M.K., Babale, S.A., Chattha, H.T., Himdi, M., Raza, A., Younas, M., Rahman, T.A., Rahim, S.K.A. and Khawaja, B.A. (2021) 'Compact wide-angle scanning multibeam antenna array for V2X communications', IEEE Antennas and Wireless Propagation Letters, 20(11), pp. 2141–2145.

Kalteh, A.A., DadashZadeh, G.R., Naser-Moghadasi, M. and Virdee, B.S. (2012) 'Ultra-wideband circular slot antenna with reconfigurable notch band function', IET Microwaves, Antennas & Propagation, 6(1), pp. 108–112.

Khadar, S.A., Panda, N.K., Mohapatra, S. and Sahu, S. (2021) 'Design of metasurface-based printed monopole antenna for wideband applications', Proceedings of the 2nd International Conference on Intelligent Engineering and Management (ICIEM), IEEE, pp. 177–181.

Li, Z., Zhu, X. and Yin, C. (2019) 'CPW-fed ultra-wideband slot antenna with broadband dual circular polarization', AEU - International Journal of Electronics and Communications, 98, pp. 191–198.

Luo, Y. et al. (2022) 'A wideband mmWave microstrip antenna based on zero-mode and TM-mode resonances', International Journal of RF and Microwave Computer-Aided Engineering, 32(8).

Paracha, K.N., Butt, A.D., Alghamdi, A.S., Babale, S.A. and Soh, P.J. (2019) 'Liquid metal antennas: materials, fabrication and applications', Sensors, 20(1), p. 177.

Ramya, C.M. and Rani, R.B. (2022) 'Design of CPW-fed dodecagon monopole antenna for ultra-wideband applications with Hilbert curve fractal', in Communications in Computer and Information Science, pp. 731–736.

Shakib, M.N., Islam, M.T. and Misran, N. (2010) 'Stacked patch antenna with folded patch feed for ultra-wideband application', IET Microwaves, Antennas & Propagation, 4(10), pp. 1456–1461.

Singhal, S. and Singh, A.K. (2016) 'CPW-fed 8-shaped monopole antenna for ultra wideband applications', Frequenz, 70(11–12), pp. 479–489.

Toktas, A. and Turkmen, H.A. (2023) 'Ultra-wideband monopole antenna with defected ground for millimeter-wave applications', Journal of Infrared, Millimeter, and Terahertz Waves, 44(1–2), pp. 37–51.

Yen, S., Boskovic, L.B., Elmansouri, M.A. and Filipovic, D.S. (2023) 'Ultra-wideband directional electrically small antenna for UHF through C-band 5G and beyond 5G applications', Microwave and Optical Technology Letters, May.

Zhu, Y., Chen, K., Tang, S.Y., Yu, C. and Hong, W. (2023) 'Ultra-wideband strip-loaded slotted circular patch antenna array for millimeter-wave applications', IEEE Antennas and Wireless Propagation Letters, pp. 1–5.